Original Article

Unraveling morphology, methylation profiling, and diagnostic challenges in BRAF-Mutant pediatric glial and glioneuronal tumors

Murad Alturkustani, *MBBS, FRCPC.*

ABSTRACT

الأهداف: توضيح العلاقة بين تحديد مثيلة الحمض النووي (DMP) والتشخيص المرضي (PD) في الأورام الدبقية والعصبية الدبقية لدى الأطفال مع طفرات الجين الورمي البروتيني، وطفرات سيرين / ثريونين كيناز (BRAF)، ومعالجة التحديات التشخيصية الخاصة بهم.

المنهجية: أجريت هذه الدراسة الاستعادية، التي أجريت في المملكة العربية السعودية، بتحليل 47 حالة من قاعدة البيانات الإلكترونية لشبكة أورام دماغ الأطفال باستخدام الصور الممسوحة ضوئيًا وبيانات تسلسل الجيل التالي وملفات تعريف المثيلة التي تمت معالجتها باستخدام مصنفات ورم الدماغ بمثيلة هايدلبرغ v12.5 و v12.8. تم الوصول إلى البيانات آخر مرة في 10 نوفمبر 2023.

النتائج: لوحظ أعلى معدل انتشار لطفرات *BRAF* في الورم النجمي الشعري والورم الدبقي العقدي. كان DMP متسقًا مع PD في 23 حالة، ولكن ظهرت تناقضات في حالات أخرى، بما في ذلك التغيرات التشخيصية في الورم العصبي الدبقي السحائي المنتشر والورم الظهاري العصبي متعدد الأشكال منخفض الدرجة لدى الشباب. ظهر تناقض رئيسي بين ورم النجمي الشعري MC وورم عصبي دبري PD. تم تصنيف اثنين من الأورام النجمية عالية الجودة بشكل خاطئ على أنها ورم صفراوي نجمي متعدد الأشكال. بالإضافة إلى ذلك، من المحتمل أن يكون التردد الأليلي المنخفض في الأورام الدبقية العقدية قد ساهم في التصنيف الخاطئ كعنصر تحكم في 5 حالات.

الخلاصة: أكدت هذه الدراسة على أهمية دمج DMP مع PD في تشخيص الأورام الدبقية والعصبية الدبقية لدى الأطفال مع طفرات *BRAF*. على الرغم من أن DMP يقدم رؤى تشخيصية مهمة، إلا أن حدوده، خاصة في الحالات التي يكون فيها محتوى الورم منخفضًا، تتطلب تفسيرًا حذرًا، فضلاً عن استخدامه كأداة تشخيصية تكميلية، بدلاً من كونه طريقة نهائية.

Objectives: To elucidate the relationship between DNA methylation profiling (DMP) and pathological diagnosis (PD) in pediatric glial and glioneuronal tumors with B-Raf proto-oncogene, serine/threonine kinase *(BRAF)* mutations, addressing their diagnostic challenges.

Methods: This retrospective study, conducted in Saudi Arabia, analyzed 47 cases from the Children's Brain Tumor Network online database using scanned images, next-generation sequencing data, and methylation profiles processed using the Heidelberg methylation brain tumor classifiers v12.5 and v12.8. The data was last access on 10 November 2023.

Results: The highest prevalence of *BRAF* mutations was observed in pilocytic astrocytoma and ganglioglioma. The DMP was consistent with PD in 23 cases, but discrepancies emerged in others, including diagnostic changes in diffuse leptomeningeal glioneuronal tumor and polymorphous low-grade neuroepithelial tumor of the young. A key inconsistency appeared between a pilocytic astrocytoma MC and a glioneuronal tumor PD. Two high-grade astrocytomas were misclassified as pleomorphic xanthoastrocytomas. Additionally, low variant allelic frequency in gangliogliomas likely contributed to misclassifications as control in 5 cases.

Conclusion: This study emphasized the importance of integrating DMP with PD in diagnosing pediatric glial and glioneuronal tumors with *BRAF* mutations. Although DMP offers significant diagnostic insights, its limitations, particularly in cases with low tumor content, necessitate cautious interpretation, as well as its use as a complementary diagnostic tool, rather than a definitive method.

Neurosciences 2024; Vol. 29 (3): 168-176
doi: 10.17712/nsj.2024.3.20230108

From the Department of Pathology, King Abdulaziz University, Jeddah, Kingdom of Saudi Arabia, and from the Department of Pathology and Laboratory Medicine, Western University, London, ON, Canada

Received 17th November 2023. Accepted 9th May 2024.

Address correspondence and reprint request to: Dr. Murad Alturkustani, Department of Pathology, King Abdulaziz University, Jeddah, Kingdom of Saudi Arabia. E-mail: alturkustani.murad@gmail.com
ORCID ID: https://orcid.org/0000-0003-4922-4112

The spectrum of differential diagnosis for BRAF-mutant pediatric glial and glioneuronal tumors spans central nervous system (CNS) world health organization (WHO) grade 1–4 tumors. Ensuring accurate diagnosis of these unique tumor types can occasionally be daunting. With its innovative approach, DNA methylation profiling's (DMP) role as an essential tumor classification tool has been confirmed. Although DMP provides invaluable advantages—especially when conventional diagnostic avenues fall short—it is essential to recognize its inherent limitations. The DMP's essence lies in its ability to analyze DNA methylation patterns within tumors and juxtapose these with a reference database, thus enhancing tumor-type identification accuracy.

Pathological diagnosis (PD) combines molecular findings with the conventional histological method to provide a final diagnosis. In contrast, methylation profiling establishes a methylation class, which remains separate from histological attributes. The resulting alignment of a methylation profile with a PD can either be in harmony (concordant) or at odds (discordant). When a variance arises between the 2, deciding which method holds precedence is necessary. The need for consensus when navigating such scenarios presents a challenge.

Prior research has focused mainly on comparing histological diagnosis and DMP classes across a broad spectrum of CNS tumors.[1–4] However, focusing specifically on *BRAF*-mutant tumors, this study offers a sharper, more nuanced analysis, highlighting the intricacies and hurdles inherent in discordant cases. This refined lens aims to underscore DMP's distinct advantages in a specific context.

Assessing DMP's utility in diagnosing *BRAF*-mutant pediatric glial and glioneuronal tumors and emphasizing navigation of the intricate terrains of discordant cases were central to this investigation. Through an in-depth analysis of its applicability and efficacy, the goal was to underscore DMP's intrinsic value, particularly when faced with the limitations of traditional diagnostic measures. Gaining a comprehensive understanding of DMP's inherent challenges and limitations is crucial for managing such cases.

Methods. This study, conducted in Saudi Arabia, gathered cases classified as glial or glioneuronal tumors with BRAF mutations from the Children's Brain Tumor Network (CBTN) online database. The available database was part of an online database accessible at https://pedcbioportal.kidsfirstdrc.org. The CBTN protocol indicated that consent was acquired from all participants or their representatives. This study's starting cohort comprised 50 cases (56 samples). The inclusion criteria were: (1) either the initial diagnosis or representative scanned images were available; (2) next-generation sequencing (NGS) data were accessible; and (3) the raw methylation profile file was present. The Heidelberg methylation brain tumor classifier (v12.5) was employed to delineate tumors' molecular classes. Accessible via the Molecular Neuropathology website (https://www.molecularneuropathology.org/mnp), this classifier provided methylation profiling results that included each tumor's methylation class (MC) along with its corresponding score and copy number profile. In this study, the calibration score 0.84 was employed as the family/case score cutoff, similar to the previous study.[3] As the v12.8 classifier was released during this project, selected cases were reanalyzed using the updated v12.8 classifier; results from both versions were compared. The data was last accessed on 10 November 2023.

The PD was carried out by integrating information from the pathology report, encompassing a comprehensive description and the preliminary histological diagnosis, reviewing available representative scanned slides and the existing molecular results, and adhering to the WHO 2021 diagnostic criteria, as applicable. Three cases were omitted from the analysis; 2 were omitted due to inadequate data, and a third had a *BRAF* mutation within a hypermutated tumor. After these exclusions, the remaining 47 cases that met the selection criteria comprised 25 males and 22 females. These participants ranged from as young as four months to 20 years, averaging approximately 9.8 years. A wide array of PDs were observed: 17 gangliogliomas (GG), 14 pilocytic astrocytomas (PA), 7 pleomorphic astrocytomas (PXA), 4 high-grade astrocytomas, 2 low-grade glial/glioneuronal tumors (GNT), 2 desmoplastic infantile astrocytoma/ganglioglioma (DIA/G), and one low-grade astrocytoma. The most frequently observed *BRAF* mutation was *BRAF* p.V600E (c.1799T>A), which was detected in 43 cases. Other identified *BRAF* alterations included *BRAF* A598_T599insV, *BRAF* V600Dfs*, *BRAF* L410Q, and *BRAF* T599dup.

The DMP's utility was evaluated by juxtaposing the PD with the MC, leading to the formation of 3 primary categories. The first was "Concordant," in which the PD aligned with the MC, resulting in either a congruence in diagnosis or a minor refinement based on the MC. The second primary category was "Discordant," which

had 3 subcategories. In the "Diagnosis Modifying" subcategory, the final diagnosis leaned towards the MC rather than the PD. In the "Misleading" subcategory, the final diagnosis adhered to the PD despite a differing MC with a high calibration score (above 0.84), but excluded instances with an MC of "control tissues." The "Debatable" subcategory was applied when the MC deviated from the PD without drawing a definitive conclusion about the final diagnosis. The third primary category, "Non-contributory," encompassed cases with a calibration score less than 0.84 and those in which the MC indicated "control tissue" with a higher calibration score. In the latter situation, as the morphological features aligned with a tumor, and every case in the study had a *BRAF* mutation, this scenario likely hinted at sampling issues during molecular tests. This nuanced classification method offered a distinct approach from what was employed in past studies.[1,3] Cases falling within the "Discordant" and "Non-contributory" categories underwent a detailed analysis to address the discrepancies and determine the optimal diagnostic path.

Results. Table 1 summarizes clinical and molecular data for the studied cases. The influence of methylation profiling on final diagnoses varied: it confirmed 23 cases, altered 2 diagnoses, resulted in contentious outcomes for 8 cases, was misleading in 2 instances, and had no contributory value in 12 cases.

In the "Concordant" category, methylation profiling confirmed initial diagnostic impressions for 23 cases. These included 12 pilocytic astrocytomas, 4 gangliogliomas, and 7 pleomorphic xanthoastrocytomas. The morphological features of these tumors were typical of their respective diagnoses, and methylation profiling served to reinforce the PDs.

The diagnosis-modifying subcategory comprised 2 cases in which methylation profiling prompted a reconsideration of the PD. Revised diagnoses occurred in cases in which the initial evaluation overlooked the most probable diagnosis, most likely due to limited exposure to recently defined tumor entities in the CNS WHO classification of tumors. However, upon reevaluation considering the newly suggested diagnosis associated with the methylation class, it became evident that the methylation class was indeed more accurate.

Case 24 pertained to a spinal cord tumor removed from a 3-year-old girl. The PD was a pilocytic astrocytoma based on the morphological presence of a biphasic tumor with areas containing piloid cells and Rosenthal fibers (**Figure 1A**) and an area formed by oval to elongated tumor cells, but without eosinophilic granular bodies (EGBs) (**Figure 1B**). However, the methylation class indicated a diffuse leptomeningeal glioneuronal tumor (DLGNT), subtype 1, with a calibration score (CS) of 0.99. Furthermore, the tumor's copy number profile revealed a 1p loss with no 1q gain. Reevaluation of the morphological features showed that they indeed fell within the DLGNT spectrum. The final diagnosis was changed to DLGNT, bumping the CNS WHO grade to at least 2. In Case 25, the PD was ganglioglioma (GG), as the morphology showed the presence of dysmorphic ganglion cells (**Figure 1C**) and an oligodendroglia-like area as the glial component (**Figure 1D-F**). The methylation class, however, suggested polymorphous low-grade neuroepithelial tumor of the young (PLNTY), with a 0.98 calibration score for the family of low-grade glial/glioneuronal/neuroepithelial tumors and a 0.73 calibration score for the PLNTY methylation class. Given that the morphological features fit within the PLNTY spectrum, the final diagnosis was subsequently revised to PLNTY.

Eight cases (Cases 26–33) presented conflicting PD and methylation class results. Methylation classes identified these tumors as pilocytic astrocytomas, whereas PDs classified them differently, as gangliogliomas (Cases 26–31) and desmoplastic infantile astrocytoma/ganglioglioma (Cases 32 and 33). Upon reevaluation, many dysmorphic ganglion cells were affirmed in all ganglioglioma instances (**Figure 2A–F**), favoring PD classifications over methylation classes. For Cases 32 and 33, leptomeningeal desmoplastic reactions were observed alongside low-grade astrocytoma components, but without any embryonal elements, and with an absence of Rosenthal fibers. Sparse dysmorphic ganglion cells and rare eosinophilic granular bodies were present in Case 33, but absent in Case 32. The PD designations for both cases were reliant on observed desmoplastic reactions. However, the possibility of pilocytic astrocytoma accompanied by a desmoplastic leptomeningeal reaction could not be dismissed entirely, leading to the inclusion of these cases in this subcategory.

Notably, the pilocytic astrocytoma with gangliocytic differentiation category could accommodate the presence of dysmorphic ganglion cells. This category was usually linked to cerebellar examples with KIAA1549-*BRAF* fusion. Five of the 6 cases in this category were supratentorial, and one was cerebellar. Given that ganglioglioma and pilocytic astrocytoma activate the

mitogen-activated protein kinase (MAPK) pathway, it was rational to keep this diagnostic possibility open pending further investigation, and is examined in more detail in the discussion section.

Methylation profiling proved misleading in 2 cases (Cases 34 and 35), suggesting pleomorphic xanthoastrocytomas despite PDs that indicated high-grade astrocytomas. Reevaluation (**Figure 3A–F**) did not reveal characteristics to support the methylation profiling class; the behavior of these tumors was more consistent with their PDs, given their survival periods of 18 and 16 months, respectively.

The non-contributory category (cases with a calibration score below 0.84 or a methylation class of "control tissue") included 12 cases (Cases 36–47). Seven of these cases were identified as "control tissue" according to their methylation classes, 3 of which had a calibration score exceeding 0.84. The PD for 5 of these 7 cases was ganglioglioma; the remaining 2 cases were low-grade astrocytoma and pilocytic/pilomyxoid astrocytoma. The remaining 5 of 12 cases in the non-contributory category included 2 high-grade astrocytomas, 2 low-grade glial/glioneuronal tumors, and one ganglioglioma.

For Cases 36–45, the PDs consisted of 6 gangliogliomas, one midline glioma, one high-grade astrocytoma, one low-grade astrocytoma, and one pilocytic astrocytoma. In the last 2 cases (Cases 46–47), the PDs were descriptive (i.e., low-grade glial vs. glioneuronal tumor). Case 46 featured a predominantly infiltrative tumor (**Figure 4A**) with pleomorphic cells and dysmorphic ganglion cells (**Figure 4B**), and exhibited diffuse positivity for CD34 immunostaining (**Figure 4C**) without any high-grade features. The differential diagnosis considered diffuse astrocytoma, ganglioglioma, and pleomorphic xanthoastrocytoma (PXA). The methylation class was categorized as low-grade ganglioglial/neuroepithelial tumor (0.76) and ganglioglioma (0.52). The copy number profile in the methylation profile showed no evidence of *CDKN2A/B* loss. As such, the final diagnosis was ganglioglioma.

In Case 47, the tumor exhibited solid and infiltrative components (**Figure 4D**). Some neoplastic cells were pleomorphic, and EGBs were present (**Figure 4E**). Although PXA was the most likely diagnosis, the presence of binucleated dysmorphic ganglion cells (**Figure 4F**) also suggested the possibility of ganglioglioma. The copy number profile in the methylation profile showed *CDKN2A/B* loss. The methylation class was identified as diffuse glioma, MAPK-altered, Cell Cycle Activated (0.60), and PXA-like (0.52). The final diagnosis was PXA, based on the tumor's morphology and copy number profile, not the methylation class. As the diagnosis modification was based on the copy number profile and not the methylation class, this case remained in the non-contributory category.

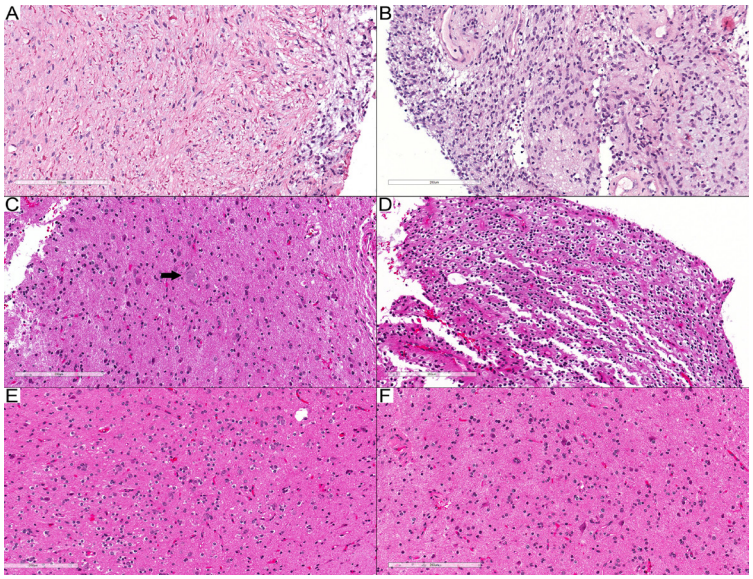

Figure 1 - Tumors with modified diagnoses. **A, B)** Case 24: DLGNT. **A)** Biphasic tumor with piloid glial cells and numerous Rosenthal fibers. **B)** Glial component with round to oval nuclei. **C–F)** Case 25: PLNTY. **C)** Dysmorphic ganglion cell (arrow). **D)** Oligodendroglioma-like component. **(E, F)** Infiltrative component. Scale bars: 200 µm (**A–F**).

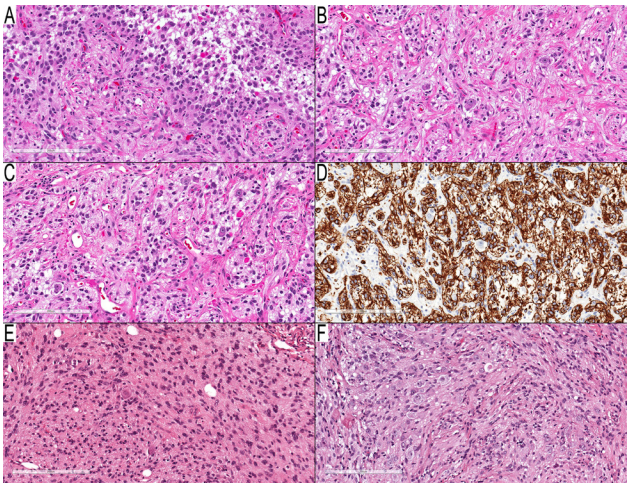

Figure 2 - Tumors with debatable diagnoses. **A–D**) Case 29: temporal lobe mass in a three-year-old boy. **A**) Neoplastic cells with round and elongated nuclei and many EGBs. **B, C**) Many dysmorphic ganglion cells with binucleated form in (**C**). **D**) Diffusely positive GFAP in the background, but negative in dysmorphic ganglion cells. **E–F**) Case 31: cerebellar tumor in a 3-year-old boy. **E**) Infiltrative components consist of elongated neoplastic cells with entrapped neurons. **F**) Many dysmorphic ganglion cells. Scale bars: 200 µm (**A–F**).

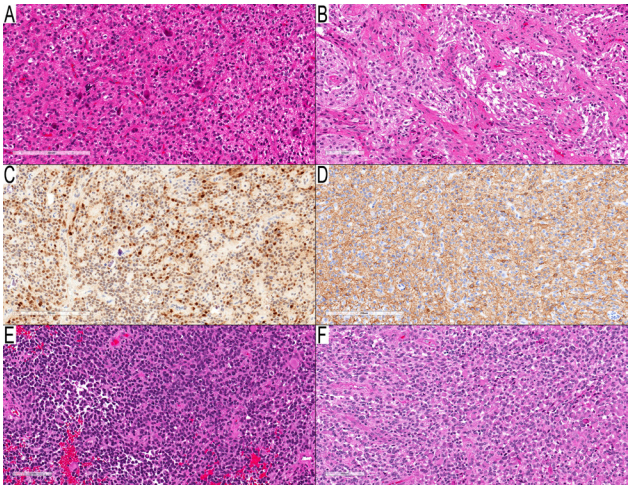

Figure 3 - Two cases with morphology of high-grade astrocytoma and MC of PXA. **A–D**) Case 34: parieto-temporal mass in a nine-year-old girl. **A**) Cellular component with round neoplastic cells infiltrative around entrapped nuclei. **B**) Two granular mitoses in the center of the field. (**C**) NeuN immunostain, an immunopositive subset of neoplastic nuclei, which raised the possibility of a neuronal component, but there was no clear neuronal differentiation. (**D**) GFAP immunostain shows a cytoplasmic rim in many neoplastic cells and the background. (**E–F**) Case 35: temporal lobe mass in a two-year-old boy. (**E**) High-cellular area with round-oval hyperchromic neoplastic cells and significant mitotic activity. (**F**) Many neoplastic cells with eccentric round eosinophilic cytoplasm resembling rhabdoid or epithelioid neoplastic cells. Scale bars: 200 µm (**A, C, D**); 100 µm (**B, E, F**).

As ganglioglioma was frequently misdiagnosed via DNA methylation profiling (DMP), often due to a low tumor content, these cases' variant allelic frequencies (AFs) were compared across different groups. In 7 cases in which ganglioglioma was misclassified as control tissue, AFs ranged from 0.07 to 0.24, with a 0.13 average, indicating a lower frequency spectrum. Conversely, 4 cases of ganglioglioma with a concordant diagnosis between methylation class and pathological diagnosis exhibited higher AFs, averaging 0.25. The independent t-test used to compare these 2 groups' AFs yielded a statistically significant *p*-value of approximately 0.040. Four ganglioglioma cases identified as pilocytic astrocytoma demonstrated a 0.22 mean AF. The independent t-test used to compare this group's AFs with those of the group of 4 ganglioglioma

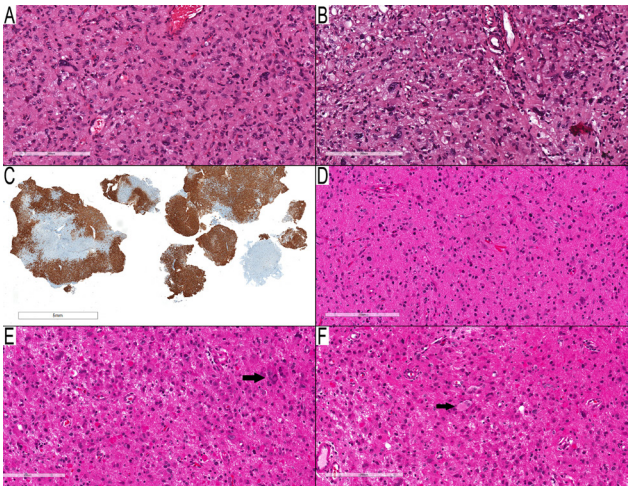

Figure 4 - Examples of cases in the non-contributary category. **A–C**) Case 46: parietal lobe mass in a thirteen-year-old woman. **A**) Spindled neoplastic cells infiltrate around entrapped neurons with scattered pleomorphic neoplastic cells. **B**) Scattered dysmorphic ganglion cells, but no EGBs present. **C**) CD34 immunostaining shows diffuse staining in the neoplastic cells. **D–F**) Case 47: occipital/temporal lobe mass in an eleven-year-old girl. **D**) Infiltrative glial component with round to slightly elongated nuclei. **E**) Area with many EGBs and scattered pleomorphic ganglion cells. (**F**) A rare example of a binucleated dysmorphic ganglion cell (arrow). Scale bars: 200 µm (**A, B, C–F**); 5 mm (**C**).

cases with concordant diagnosis between methylation class and pathological diagnosis yielded a statistically insignificant *p*-value of approximately 0.648.

Discussion. This research examined the synergy between MC and PD, specifically within the scope of pediatric glial and glioneuronal tumors harboring *BRAF* mutations. Within this tumor spectrum, DMP application provided distinct advantages in 2 of 47 cases, culminating in a diagnostic shift, and sparked a contentious debate regarding the morphological range of pilocytic astrocytoma in 8 cases. The DMP aligned with PD was potentially misleading in 2 of 23 cases, and remained inconclusive in 12 cases. Cases of discordance are elaborated on in the following discussion.

One significant finding was the prevalence of the *BRAF* mutation in pediatric glial and glioneuronal tumors. Excluding debatable cases from this cohort, PA was identified as the predominant tumor possessing a *BRAF* mutation (14/39; 35.8%), followed closely by ganglioglioma (10/39; 25.6%) and PXA (8/39; 20%). When including contentious cases and accepting PD as the final diagnosis, ganglioglioma was the most prominent tumor type (16/47; 34.0%), followed by pilocytic astrocytoma and PXA. This distribution differed from results reported in the literature, especially when juxtaposed against a study of 96 *BRA*F mutant tumors from 1320 adult and pediatric cases. In that study, PXA was the primary *BRAF* mutant tumor spanning both grades (57/1320; 4%), followed by ganglioglioma (14/1320; 1%) and PA (9/1320; 0.6%).[5] Nonetheless, our results mirror those of Horbinski et al,[6] who noted that 10 of 19 cases of low-grade gliomas with *BRAF* V600E were pilocytic astrocytomas, one was a pilomyxoid astrocytoma, 5 were gangliogliomas, 2 were PXAs and one was a low-grade diffuse glioma.[6] Therefore, although our results indicate that PXA had the highest *BRAF* V600E percentage and pilocytic astrocytoma had the lowest percentage, statistically, a brain tumor with *BRAF* V600E is more likely to be a pilocytic astrocytoma or ganglioglioma than a PXA.

The 2 cases in which DMP led to a revision of the PD, resulting in more precise diagnoses of DLGNT and PLNTY, indicated DMP's role in revealing less-recognized or newly-established entities. Even though these cases presented overlapping histological features and molecular alterations, the proper use of morphological and molecular data could have initially led to an accurate diagnosis. The first case was particularly notable; the diagnosis shifted from a CNS WHO grade 1 pilocytic astrocytoma to a DLGNT (CNS WHO grade 2). The DLGNT should demonstrate diffuse synaptophysin staining and restricted GFAP expression, if present,[7] whereas PA should display widespread GFAP staining.[8] Additionally, DLGNT usually shows a loss of 1p, as it did in this case. The second case might have posed more of a challenge, as ganglioglioma and PLNTY share numerous features,

including oligodendroglioma-like areas, diffuse CD34 immunostaining, and BRAF alterations. Diffuse infiltration, a characteristic more typical of PLNTY, has also been described in ganglioglioma.[9] The presence of dysmorphic ganglion cells was more likely to indicate the possibility of ganglioglioma; however, sporadic or scarce cells of this type have been reported in various tumors.[10]

There were 8 cases in the debatable category, in which a recurring pattern emerged; tumors classified as pilocytic astrocytomas via DMP contrasted with PDs of ganglioglioma (6 cases) or desmoplastic infantile astrocytma/ganglioglioma (2 cases). These observations opened the door for further investigation into the morphological spectrum of pilocytic astrocytomas.

The literature presents this debate by highlighting difficulties differentiating between pilocytic astrocytoma and ganglioglioma. One group posits that some infratentorial gangliogliomas should be regarded as pilocytic astrocytomas with ganglionic differentiation.[11] In supratentorial (especially temporal lobe) tumors with pilocytic astrocytoma morphology and *BRAF* V600E, mutation might recur with more frequent dysmorphic ganglion cells. As a result, another group favors a ganglioglioma diagnosis for such tumors.[12] As DNA methylation profiling patterns echo the cell of origin,[13] and different methylation classes for pilocytic astrocytoma, ganglioglioma, and desmoplastic infantile glioma are present in the system, the methylation class of pilocytic astrocytoma for these tumors supports the position that they differ from classic cases. This issue is also prominent in the DMP, as "classifier"v11.4 hosted a class named "methylation class low-grade glioma, subclass hemispheric pilocytic astrocytoma, and ganglioglioma," reflecting the uncertainty in distinguishing between these 2 tumor types. In the revised v12.5 version, the term "ganglioglioma" was omitted, and the class evolved into "MC Pilocytic astrocytoma, hemispheric."

Reevaluation of these debatable cases confirmed the presence of many dysmorphic ganglion cells, but revealed no significant features that lead to a change in the PD. However, for the above reasons, these cases were included in the debatable subcategory, leaving the possibility of further investigation into such tumors. The suggested debate should not have significant clinical implications if targeted therapy was warranted, as all 3 tumors were considered CNS WHO grade 1 and exhibited similar mutations.

Classification challenges arose in 4 cases: 2 in the discordant category (Cases 34 and 35) and 2 in the non-contributory category (Cases 46 and 47), particularly regarding diagnosing PXA. The challenges in Cases 34 and 35 pertained to PXA's broad MC spectrum. These 2 cases were discussed in more detail in previous study.[14] The literature has recognized this limitation, as this class can encompass cases with histological diagnoses ranging from diffuse glioma, glioneuronal tumors to GBM-like and ATRT-like tumors.[3] Although the final diagnosis for these cases leaned towards the PD of grade 4 astrocytoma, supported by unfortunate outcomes, this category remains ambiguous. In this study, MC PXA demonstrated sensitivity in the detection of all PXA cases; however, another study found that it misclassified 6 of 67 histologically defined PXAs.[15]

Cases 46 and 47 presented challenges in distinguishing between PXA and its frequently encountered differential diagnosis, ganglioglioma, mainly when PXA-like components were observed in the glial fraction of ganglioglioma.[16] The 2 entities shared several histological characteristics, exhibited CD34 immunostaining, and showed MAPK activation via the *BRAF* V600E mutation. CDKN2A/B homozygous loss was a distinguishing feature characteristic of PXA.[16] Additionally, the presence of "true" dysmorphic ganglion cells aligned with a ganglioglioma diagnosis, as PXA might present neurocytic differentiation immunohistochemically, but not in morphological terms.[16] The PD for these 2 cases were low-grade glial or glioneuronal tumors, with differential diagnoses of PXA and ganglioglioma. Methylation classes were inconclusive, but the DMP report's CDKN2A/B status was decisive. The lack of CDKN2A/B loss in Case 46 led to a ganglioglioma diagnosis, whereas CDKN2A/B loss in Case 47 was consistent with PXA.

The non-contributory category was divided into 2 subsets. The first subset consisted of cases in which the MC was identified as control tissue, irrespective of its score; the second subset involved cases with family and class scores below 0.84. In the first subset, 3 of 7 cases labeled as control tissue scored above 0.84. Ganglioglioma was the predominant PD, accounting for 5 of the 7 cases, succeeded by a single case of pilocytic/pilomyxoid and low-grade astrocytoma. This pattern aligned with existing literature regarding ganglioglioma, particularly in cases with minimal tumor content.[3] Other reasons for a methylation classification of "control" tissue might include the diffuse glioma's infiltrative zone or highly inflammatory tumors.[3] In this study, the variant AF analysis offers valuable insights into the diagnostic challenges associated with DMP in cases of ganglioglioma. Gangliogliomas misclassified as

Table 1 - Summary of clinical and molecular characteristics of studied cases.

No.	Age (Y)	Sex	Site	PD	NGS	AF	MC V12.5	MC V12.8	Final diagnosis
1	1.7	M	OP	PA	*BRAF* V600E	0.29	PA-M (0.99)	PA-M (0.99)	PA
2	7	F	Ce	PA	*BRAF* A598_T599insV	0.31	PA-I (0.99)	PA-I (0.99)	PA
3	17	M	TL	PA	*BRAF* V600Dfs*47	0.08	PA-H (0.89)	PA-H (0.79)	PA
4	11	M	FL;PL	PA	*BRAF* V600E	0.19	PA-H (0.93)	PA-H (0.96)	PA
5	12	F	OP	PA	*BRAF* V600E	0.13	PA-M (0.99)	PA-M (0.99)	PA
6	15	M	Ce	PA	*BRAF* L410Q	0.22	PA-I (0.99)	PA-I (0.99)	PA
7	1.6	M	TL	PA	*BRAF* V600E	0.28	PA-H (0.98)	PA-H (0.81)	PA
8	15	M	OP	PA	*BRAF* V600E	0.15	PA-M (0.99)	PA-M (0.99)	PA
9	15	M	Ce	PA	*BRAF* T599dup, Ad1	0.48	PA-I (0.89)	PA-M (0.59)	PA
10	1.2	M	OP	PA	*BRAF* V600E	0.2	PA-M (0.99)	PA-M (0.98)	PA
11	14	F	BS	PA-R	*BRAF* T599dup	0.59	PA-I (0.98)	PA-I (0.90)	PA
12	16	M	TL	PA	*BRAF* V600E	0.26	PA-H (0.94)	PA-H (0.98)	PA
13	14	F	TL	GG	*BRAF* V600E	0.24	GG (0.99)	GG (0.99)	GG
14	0.75	F	TL	GG	*BRAF* V600E	0.18	GG (0.94)	GG (0.98)	GG
15	2	M	TL	GG	*BRAF* V600E	0.18	GG (0.75)	GG (0.85)	GG
16	3	M	TL	GG	*BRAF* V600E	0.41	GG (0.99)	GG (0.99)	GG
17	14	F	TL	PXA	*BRAF* V600E	0.36	PXA (0.99)	PXA (0.99)	PXA
18	13	M	TL	PXA	*BRAF* V600E	0.48	PXA (0.99)	PXA (0.99)	PXA
19	9	F	FL	PXA	*BRAF* V600E	0.51	PXA (0.99)	PXA (0.99)	PXA
20	14	F	FL	PXA	*BRAF* V600E	0.29	PXA (0.99)	PXA (0.99)	PXA
21	14	M	TL	PXA	*BRAF* V600E	0.41	PXA (0.99)	PXA (0.99)	PXA
22	10	M	PL	PXA	*BRAF* V600E	0.3	PXA (0.99)	PXA (0.99)	PXA
23	12.3	F	TL	As- Inf	*BRAF* V600E	0.3	GG (0.50)	GG (0.80)	LG GNT vs As
23	16.3	F	Hip	PXA	*BRAF* V600E	0.24	PXA (0.99)	PXA (0.99)	PXA
24	3.6	F	SC	PA	*BRAF* V600E	0.49	DLGNT-1 (0.99)	DLGNT-1 (0.99)	DLGNT
25	13.9	F	TL	GG	*BRAF* V600E	0.69	PLNTY (0.73)	PLNTY (0.48)	PLNTY
26	18	M	TL	GG	*BRAF* V600E	0.12	PA-H (0.83)	PA-H (0.97)	GG
27	19	F	OL;TL	GG	*BRAF* V600E	0.19	PA-H (0.94)	PA-H (0.81)	GG
28	10	M	TL	GG	*BRAF* V600E	0.14	PA-H (0.82)	GG (0.32)	GG
29	3	M	TL	GG	*BRAF* V600E	0.38	PA-H (0.99)	PA-H (0.99)	GG
30	15	F	TL	GG	*BRAF* V600E	0.19	PA-H (0.85)	PA-H (0.99)	GG
31	3	M	Ce	GG	*BRAF* V600E	0.29	PA-I (0.99)	PA-I (0.95)	GG
32	0.25	F	OP	DIA	*BRAF* V600E	0.28	PA-M (0.99)	PA-M (0.99)	DIA vs PA
33	6	M	OP	DIG	*BRAF* V600E	0.34	PA-M (0.99)	PA-M (0.99)	PA vs DIG
34	9	F	PL;TL	HG As	*BRAF* V600E	0.46	PXA (0.99)	PXA (0.99)	pHGG, NEC
35	2	M	TL	HG As	*BRAF* V600E	0.89	PXA (0.99)	PXA (0.98)	pHGG, NEC
36	11	F	TL	GG	*BRAF* V600E	0.07	C-RM (0.56)	C-IM (0.43)	GG
37	14	M	FL	GG	*BRAF* T599dup IF ins	0.24	C-RM (0.64)	C-RM (0.46)	GG
38	4	M	BS	GG	*BRAF* V600E	0.15	C-RM (0.38)	C-RM (0.44)	GG
39	4	F	FL	GG	*BRAF* V600E, Ad2	0.09	C-RM (0.74)	C-RM (0.54)	GG
40	2	M	TL	GG	*BRAF* V600E	0.18	PA-H (0.45)	PA-H (0.57)	GG
41	16	M	TL	GG	*BRAF* V600E	0.08	C-RM (0.98)	C-RM (0.86)	GG
42	20	F	BS	LG As	*BRAF* V600E	0.11	C-RM (0.98)	C-RM (0.96)	LG As
43	11	F	PL;TL	PA/PMA	*BRAF* V600E	0.16	C-RM (0.99)	C-RM (0.97)	PA/PMA
44	9	M	TL	HG As, NEC	*BRAF* V600E, Ad3	0.53	pHGG, RTK1 (0.38)	DPHGG, RTK1 (0.47)	pHGG, NEC
45	11	F	Th	DMG, K27M	*BRAF* V600E, Ad4	0.16	G-IDHw-M (0.43)	C-IM (0.88)	DMG, K27M
46	13	F	PL	LG G/GN	*BRAF* V600E	0.33	GG (0.52)	PA-H (0.24)	GG
47	11	F	OL;TL	LG G/GN	*BRAF* V600E	0.26	PXA (0.52)	PXA (0.36)	PXA

Ad: additional mutations [Ad1: P53 X307_splice and CDH1 X177_splice; Ad2: NF1 C1792*; Ad3: TP53 R248L; Ad4: H3F3A K28M, TERT promotor mutation (not specified)]. AF: allelic frequency; BS: brainstem; C-IM: control tissue, inflammatory microenvironment; C-RM: control tissue, reactive tumor microenvironment; Ce: cerebellum; DLGNT-1: diffuse leptomeningeal glioneuronal tumor, subtype 1; F: female; FL: frontal lobe; G-IDHw-M: glioblastoma, IDH-wildtype, mesenchymal type; Hip: hippocampus; LV: lateral ventricle; M: male; ND: not done; NEC: not elsewhere classified; OL: occipital lobe; OP: optic pathway; PA-H: pilocytic astrocytoma, hemispheric; PA-I: pilocytic astrocytoma, infratentorial; PA-M: pilocytic astrocytoma, midline; pHGG: diffuse pediatric-type high-grade glioma; PL: parietal lobe; PLNTY: polymorphous low-grade neuroepithelial tumor of the young; PXA: pleomorphic xanthoastrocytoma; SC: spinal cord; Th: thalamus; TL: temporal lobe; Y: years

control tissue displayed significantly lower AFs, with a mean of 0.13, as indicated by the statistically significant *p*-value of approximately 0.040 compared to cases with concordant diagnoses, which had a mean AF of 0.25. This finding suggests that low tumor content, as reflected in lower AFs, may be a key factor contributing to the misclassification of ganglioglioma in DMP. In such cases, histological criteria may be more suitable for diagnosing ganglioglioma, and DMP might overlook cases with low AF.

The second subset encompassed 5 cases with calibration scores under 0.84. These comprised 2 high-grade astrocytomas, one ganglioglioma, and 2 low-grade glial/glioneuronal tumors. Specifically, Case 45 pertained to a thalamic mass in an eleven-year-old female. Its morphological traits resembled those of high-grade astrocytoma; next-generation sequencing revealed mutations such as *BRAF* V600E, *H3F3A* K28M, and *TERT* promoter mutation. The PD for this case was determined to be diffuse midline glioma with H3-k27 alterations.

This study's limitations included a retrospective design and reliance on publicly available resources. Hence, some preferred immunostains were not readily available. The relatively short follow-up period and small sample size limited our ability to draw definitive conclusions regarding low-grade tumors.

In conclusion, although methylation profiling offered valuable insights for diagnosing BRAF-mutant glial and glioneuronal tumors, its limitations, including misclassification of high-grade gliomas as PXA, and the noteworthy issue of misclassification of gangliogliomas as control tissue, emphasize the importance of combining it with other diagnostic methods. A key finding was the superiority of pathological assessment over DMP in ganglioglioma cases with low variant AF. The misclassifications observed in this study underscore the need for continued DMP refinement.

Acknowledgement. *This study was made possible in part due to the Children's Brain Tumor Network (CBTN).*

References

1. Jaunmuktane Z, Capper D, Jones DTW, Schrimpf D, Sill M, Dut M, et al. Methylation Array Profiling of Adult Brain Tumours: Diagnostic Outcomes in a Large, Single Centre. ***Acta Neuropathol Commun*** 2019; 7: 24.
2. Priesterbach-Ackley LP, Boldt HB, Petersen JK, Bervoets N, Scheie, D, Ulhøi BP, et al. Brain Tumour Diagnostics Using a DNA Methylation-Based Classifier as a Diagnostic Support Tool. ***Neuropathol Appl Neurobiol*** 2020; 46: 478-492.
3. Capper D, Stichel D, Sahm F, Jones DTW, Schrimpf D, Sill, M, et al. Practical Implementation of DNA Methylation and Copy-Number-Based CNS Tumor Diagnostics: The Heidelberg Experience. ***Acta Neuropathol*** 2018; 136: 181-210.
4. Sturm D, Capper D, Andreiuolo F, Gessi M, Kölsche C, Reinhardt A, et al. Multiomic Neuropathology Improves Diagnostic Accuracy in Pediatric Neuro-Oncology. ***Nat Med*** 2023; 29: 917-926.
5. Schindler G, Capper D, Meyer J, Janzarik W, Omran H, Herold-Mende C, et al. Analysis of BRAF V600E Mutation in 1,320 Nervous System Tumors Reveals High Mutation Frequencies in Pleomorphic Xanthoastrocytoma, Ganglioglioma and Extra-Cerebellar Pilocytic Astrocytoma. ***Acta Neuropathol*** 2011; 121: 397-405.
6. Horbinski C, Nikiforova MN, Hagenkord JM, Hamilton RL, Pollack IF. Interplay among BRAF, p16, p53, and MIB1 in pediatric low-grade gliomas. ***Neuro Oncol*** 2012; 14: 777-789,
7. Perry A, Capper D, Ellison DW, Jones DTW, Reifenberger G. Diffuse Leptomeningeal Glioneuronal Tumour. In: WHO Classification of Tumours Editorial Board, editors. Central nervous system tumours; WHO classification of Tumours series. Lyon (France): International Agency for Research on Cancer; 2021.
8. Alturkustani M. Diffuse GFAP Immunopositivity in the Oligodendrocyte-like Component of Pilocytic Astrocytoma Distinguishes It from Mimickers. ***Diagnostics (Basel)*** 2022; 12: 1632.
9. Alturkustani M. Classification of Pediatric Gangliogliomas Based on the Histological Infiltration. ***Curr Oncol*** 2022; 29: 6764-6775.
10. Reinhardt A, Pfister K, Schrimpf D, Stichel D, Sahm F, Reuss DE, et al. Anaplastic Ganglioglioma-A Diagnosis Comprising Several Distinct Tumour Types. ***Neuropathol Appl Neurobiol*** 2022; 48: e12847.
11. Gupta K, Orisme W, Harreld JH, Qaddoumi I, Dalton JD, Punchihewa C, et al. Posterior Fossa and Spinal Gangliogliomas Form Two Distinct Clinicopathologic and Molecular Subgroups. ***Acta Neuropathol Commun*** 2014; 2: 18.
12. Collins VP, Jones DTW, Giannini C. Pilocytic Astrocytoma: Pathology, Molecular Mechanisms and Markers. ***Neuropathol Appl Neurobiol*** 2022; 48: e12847.
13. Capper D, Jones DTW, Sill M, Hovestadt V, Schrimpf D, Sturm D, et al. DNA Methylation-Based Classification of Central Nervous System Tumours. ***Nature*** 2018; 555: 469-474.
14. Alturkustani M. Diagnostic Insights into Pediatric Pleomorphic Xanthoastrocytoma through DNA Methylation Class and Pathological Diagnosis Analysis. ***Diagnostics (Basel)*** 2023; 13: 3464.
15. Vaubel R, Zschernack V, Tran QT, Jenkins S, Caron A, Milosevic D, et al. Biology and Grading of Pleomorphic Xanthoastrocytoma-What Have We Learned about It? ***Brain Pathol*** 2021; 31: 20-32.
16. Giannini C, Capper D, Figarella-Branger D, Jacques TS, Jones DTW, Louis DN, et al. In WHO Classification of Tumours Editorial Board. Central nervous system tumours.; WHO classification of Tumours series.; International Agency for Research on Cancer: Lyon (France), 2021; 6: 94–99.